

Laser-induced acoustic desorption of thermally stable and unstable biomolecules

Zhipeng Huang^{a,b}, Daniel A. Horke^{a,c}, Jochen Küpper^{a,b,c,*}

^aCenter for Free-Electron Laser Science, Deutsches Elektronen-Synchrotron DESY, Notkestrasse 85, 22607 Hamburg, Germany

^bDepartment of Physics, Universität Hamburg, Luruper Chaussee 149, 22761 Hamburg, Germany

^cThe Hamburg Center for Ultrafast Imaging, Universität Hamburg, Luruper Chaussee 149, 22761 Hamburg, Germany

Abstract

We evaluated the effect of the laser-induced acoustic desorption (LIAD) process on thermally stable and unstable biomolecules. We found that the thermally labile glycine molecule fragmented following desorption via LIAD, due to the production of hot molecules from the LIAD process. We furthermore observed a rise in translational temperature with increasing desorption laser intensity, while the forward velocity was invariant with respect to the desorption laser intensity for both glycine and adenine molecules. The forward kinetic energy was in the range of the surface stress energy, which supports the previously proposed stress-induced desorption model for the laser-induced acoustic desorption process.

Keywords: Laser-induced acoustic desorption, gas-phase, biomolecules, mass spectrometry

1. Introduction

Laser-induced acoustic desorption [1] is a promising technique to bring thermally labile, light sensitive and non-volatile molecules into gas phase. It relies on samples being deposited as a thin layer on a metal foil, typical foil thickness of around 10 μm , which are then desorbed by irradiating the backside of the foil, i. e., the side without sample, with a nanosecond laser. As this method avoids direct contact between the desorption laser and sample, it is especially suitable for light-sensitive and labile samples and has been demonstrated for bringing biological systems ranging from amino acids [2–5], through peptides [6–8] and even entire viruses, bacteria and cells [9, 10] into the gas-phase. Such LIAD-based molecule sources have been applied to mass spectrometry studies [9, 11–13], gas-phase chemical reactions [14, 15], and even attosecond dynamics experiments [2–4]. They are further promising large-molecule sources for use in matter-wave interferome-

try [16, 17] and single-particle imaging experiments at free-electron lasers [18, 19].

We have previously demonstrated and characterized our newly designed LIAD source, featuring constant sample replenishment using a tape-drive to deliver fresh sample, and prepared a high-density plume of phenylalanine [5]. We observed that increasing the pulse energy of the desorption laser leads to increased fragmentation, as well as a significant increase in the translational temperature of desorbed molecules. In this contribution we investigated how the LIAD source parameters, such as desorption laser intensity and desorption-ionization timing, affected the produced molecular plume for thermally stable and thermally unstable biological molecules, using adenine and glycine as prototypical examples [20, 21]. Our results confirmed the previous assignment of a desorption model based on surface stress on sample islands deposited on the foil, as evidenced by the combination of an invariance of the molecular plume velocity on the desorption laser intensity, but an increase of the translational temperature [5, 22]. For the thermally labile glycine sample we found significant further fragmentation during the propagation in the vacuum chamber following desorption. These molecules were found to possess translational temperatures well above the

*Corresponding author

Email address: jochen.kuepper@cfe1.de (Jochen Küpper)

URL: <https://www.controlled-molecule-imaging.org> (Jochen Küpper)

decomposition threshold. If there is a full thermalization of internal and external degrees of freedom, which seems reasonable given the involved microsecond timescale desorption process, this would explain the observed fragmentation.

2. Experimental method

Detailed descriptions of our experimental setup and sample preparation method were given before [5]. Briefly, samples were deposited on the front surface of a 10 μm thick, 10 mm wide and 1 m long tantalum foil band. In order to create a stable coverage of sample on the foil, sample was aerosolized using a gas-dynamic virtual nozzle (GDVN) [23, 24] and this aerosol deposited on the foil, where it sticks and rapidly dries out. The surface coverage of adenine and glycine on the foil was around 600 nmol/cm^2 and 400 nmol/cm^2 , respectively, as determined by weighing foil bands before and after sample deposition. To desorb molecules, the back surface of the foil was irradiated by a 355 nm laser pulse with 8 ns duration at a repetition rate of 20 Hz, focused to a spot size of around 300 μm (FWHM) on the foil. Sample was constantly replenished during operation by forwarding the foil band with a velocity of $\sim 50 \mu\text{m}/\text{s}$. Desorbed molecules were ionized using strong-field ionization (SFI) induced by a focused femtosecond (40 fs) Ti:Sapphire laser focused to a spot size of around 100 μm , corresponding to typical field strengths of $4 \times 10^{13} \text{ W}/\text{cm}^2$. Produced ions were detected by a linear time-of-flight mass spectrometer (TOF-MS).

3. Results and Discussion

Typical time-of-flight mass spectra of adenine and glycine desorbed via LIAD are shown in Figure 1 and are compared to literature spectra obtained using electron-impact ionization of thermally evaporated samples [25]. Both spectra were normalized to their respective dominant ion peak, i. e., the parent ion peak at 135 u for adenine and the dominant fragment peak at 30 u for glycine. The adenine spectra clearly demonstrate the production of intact adenine in the gas-phase using LIAD, with very little fragmentation. For glycine, however, strong fragmentation was observed for both LIAD and the reference spectrum. Nonetheless, using LIAD combined with SFI a significant contribution from intact glycine was present. The mass spectra showed no

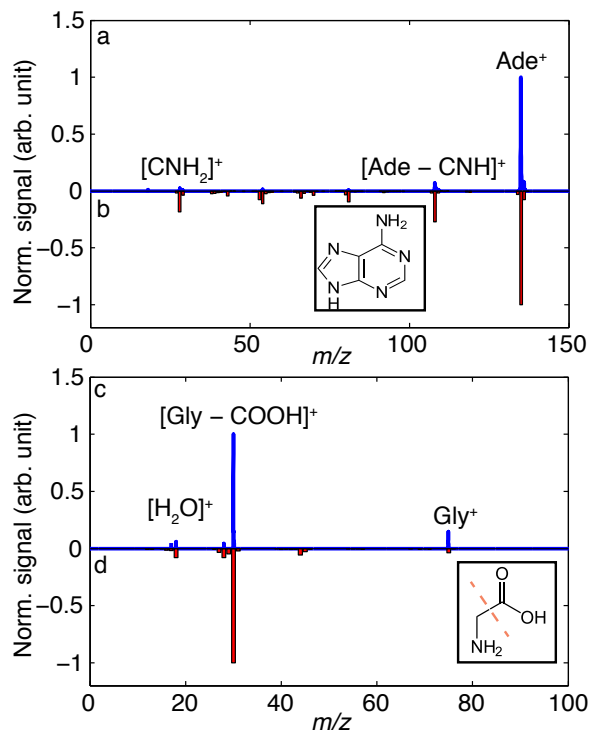


Figure 1: Mass spectrum of adenine and glycine recorded using strong-field ionization with a field strengths of $4 \times 10^{13} \text{ W}/\text{cm}^2$ (blue) and electron impact ionization (red) [25]. Both are normalized to the dominant mass-to-charge ratio peak.

evidence for the formation of molecular clusters or ablation of metal atoms or clusters from the foil band [5].

In order to investigate how the desorption laser intensity affects the fragmentation behavior for thermally stable and labile molecules, respectively, we collected mass spectra for adenine and glycine under different desorption laser intensities. Molecules were ionized using SFI 4.5 mm behind the foil band. Figure 2 a,c show the respective parent and dominant fragment ion yields as a function of desorption laser intensity. These data were fit with a power-law dependence of the form $A \times x^n$, and all ion channels showed a corresponding increase with increasing laser intensity. Figure 2 b,d shows the fragment-to-parent ratios for adenine and glycine as a function of desorption laser intensity and we observed only a slight linear increase in fragmentation as the desorption power is increased. Both thermally stable and unstable molecules, therefore, behave similar with increasing desorption laser intensity, confirming the non-thermal nature of the desorption process.

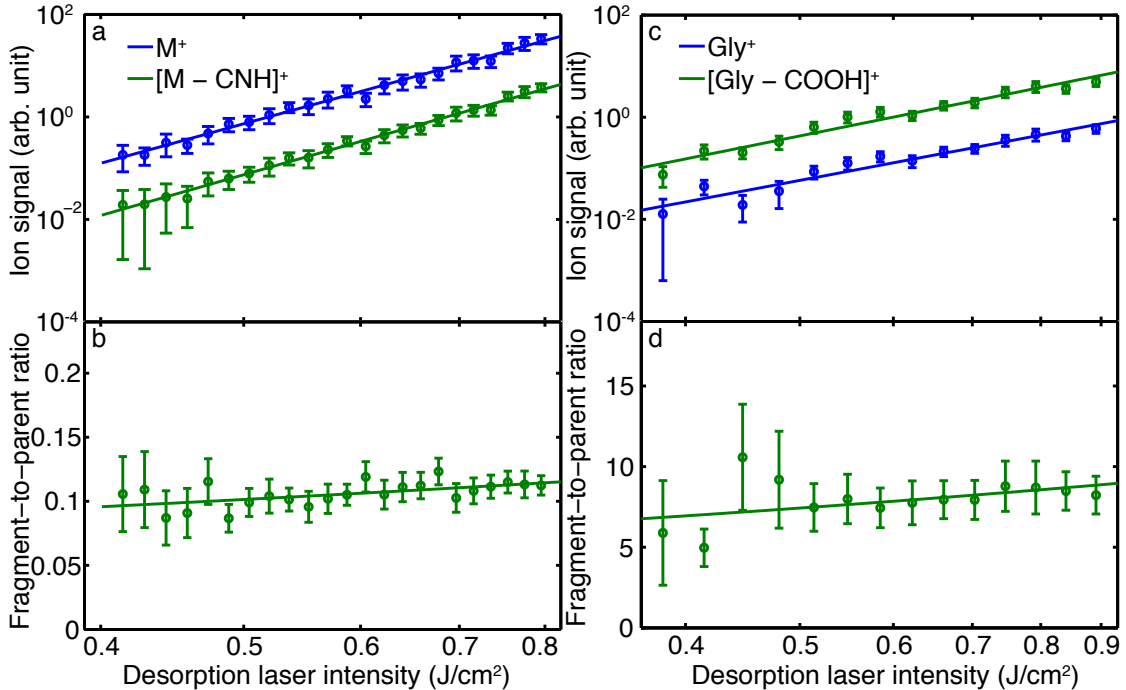


Figure 2: Parent and dominant fragment ion yields (a,c) and fragment-to-parent ratios (b,d) as a function of desorption laser intensity for adenine (a,b) and glycine (c,d). Data was recorded using strong-field ionization 4.5 mm behind the foil band.

To investigate whether further fragmentation occurred after desorption, i. e., during propagation of the molecular plume through the vacuum chamber, we recorded mass spectra at different distances behind the foil band. At each distance the delay between ionization laser and desorption laser was changed, such that we always probed the highest density part of the plume, i. e., we followed the peak of the plume as it travels. This data is shown in Figure 3 a,b, where we plot the fragment-to-parent ratio for distances of 0.5–12.0 mm between the foil band and the interaction point. Figure 3 a shows the behavior for adenine, using the dominant fragment at 108 u, corresponding to the loss of $-\text{CNH}$ from intact adenine. We observed a decrease of the fragment-to-parent ratio with distance from foil band, indicating that the peak number density of fragments decreased relatively to the adenine parent. At the same time the absolute densities for parent and fragment should decrease with increasing distance. We attribute the observed behavior to different relative velocity distributions for fragments and intact molecules. Fragments appear to be traveling at higher velocities, likely due to the additional kinetic energy released in the fragmentation process,

leading to the observed decrease in the fragment-to-parent ratio of adenine with increasing distance from the foil band. This indicates that there was no further fragmentation of adenine during propagation.

The behavior observed for glycine is markedly different, as shown in Figure 3 b. Here, the relative population of the dominant fragment at 30 u increased during propagation, indicating that further fragmentation occurred during free flight of the molecules through the chamber. We note that one might expect fragments and intact glycine to propagate at different velocities, as observed for adenine, such that the fragmentation during propagation might be even more significant than the data in Figure 3 b suggests. These two competing effects also explain the unclear variation in a corresponding measurement of the fragmentation during propagation of phenylalanine following LIAD [5]. The different behavior for adenine and glycine suggests a thermal decomposition during free flight propagation as the origin of the enhanced fragmentation. This will be investigated further below, where we assess the translational temperature of desorbed molecules.

In order to evaluate the translational forward ve-

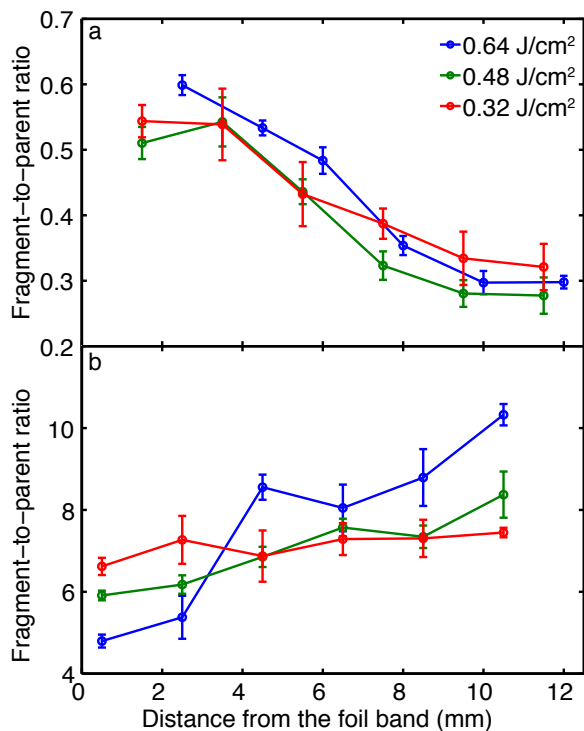


Figure 3: Fragment-to-parent ratio of adenine (a) and glycine (b) as a function of distance from the foil band for the highest density part of the plume.

locity and translational temperature of the plume, we recorded mass spectra for different ionization-desorption laser delays and at different distances from the foil. These data, shown in Figure 4, were then modeled by a Maxwell-Boltzmann distribution convoluted with the initial temporal distribution from the LIAD process [5]. The shown data was recorded for a desorption laser fluence of 0.48 J/cm^2 , profiles for other fluences are shown in the supplementary materials. All experimental data were fitted globally for all propagation distances with a common temperature T and forward velocity $v_{0,z}$. The resulting fit is shown as solid lines in Figure 4. The extracted forward velocity and translational temperature for different desorption laser intensities are summarized in Table 1. We found that the forward velocity of both, adenine and glycine, plumes was invariant with respect to desorption laser intensity, as previously observed for other molecules [5, 22]. Similarly we confirmed the previous finding that the translational temperature increases with desorption laser intensity, for both, adenine and glycine. However, while the former only shows a very modest increase over the laser fluence range investigated,

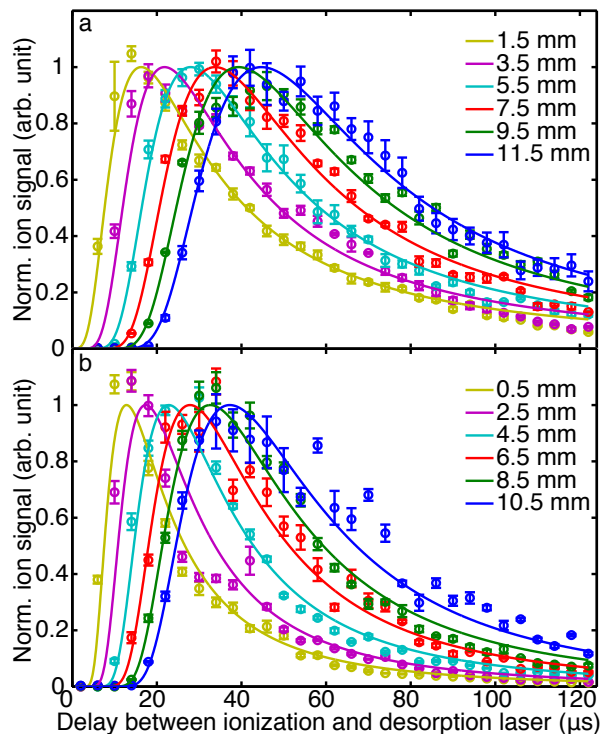


Figure 4: Adenine (a) and glycine (b) plume temporal distribution measured at different distances from the foil band for a desorption laser fluence of 0.48 J/cm^2 .

the glycine translational temperature was found to increase significantly. For all but the lowest desorption fluence, the extracted translational temperature for the glycine plume was above its thermal decomposition temperature, which is on the order of $\sim 485 - 513 \text{ K}$ [21]. The translational temperatures for adenine, however, were much below its decomposition temperature of 582 K [20]. While we have no definitive explanation for the differences in observed translational temperature, we speculate that this is due to different thermal properties, such as heat transport, from the metal foil to the sample during the desorption process. Furthermore, we note that the different thicknesses of the sample layers will influence this. Nonetheless, these results rationalize the observed fragmentation behavior following desorption from the foil band shown in Figure 3: the thermally unstable glycine fragmented further, while for adenine no additional fragmentation was observed.

The observation of a constant plume velocity, but increasing translational temperature, as well as only a modest increase in fragmentation with increasing desorption laser fluence, is a clear indicator for a des-

Table 1: Derived translational forward velocities $v_{0,z}$ and translational temperatures T in the moving frame for adenine and glycine at different desorption-laser fluences.

Fluence (J/cm ²)	Ade		Gly	
	T (K)	$v_{0,z}$ (m/s)	T (K)	$v_{0,z}$ (m/s)
0.32	494	365	441	337
0.48	516	369	496	338
0.64	521	384	698	355
0.80	523	380	745	340

orption process based on surface stress between the substrate and the deposited sample [5, 22]. The forward velocity of the molecular plume, i. e., its kinetic energy, is hence determined by material properties of the substrate and sample. From our measurements we extracted a forward kinetic energy, based on the average velocity, of around 90 meV for adenine and 45 meV for glycine. This is consistent with the previously observed kinetic energy for phenylalanine under identical conditions, around 50 meV [5], and within the range of simple estimates of the stress energy of 25–100 meV [22, 26]. The kinetic energy of desorbed molecules is essentially a measure of the interaction energy between the deposited molecules and the metal foil. In a very qualitative picture it is easy to rationalize how adenine with its highly delocalized π -system has a stronger interaction with a metal surface than glycine, with phenylalanine somewhere between the two.

4. Conclusion

We demonstrated the use of LIAD for the production of gas-phase samples of adenine and glycine, prototypical examples of thermally stable and unstable biological molecules, respectively. We showed that the high translational temperatures of molecules following desorption correlate with further fragmentation of thermally unstable systems as they travel through the vacuum chamber, indicating a strong coupling between internal and external degrees of freedom in the desorbed samples. Measurements of the translational temperature and molecular velocity distributions confirmed this, and showed that indeed glycine is produced with a temperature in excess of its decomposition threshold. The invariance of forward velocities on the desorption laser power further confirmed a desorption model based on surface stress between substrate and sample.

The additional fragmentation of molecules could be avoided if they were rapidly cooled down, for example using buffer-gas cells [27] or entrainment

in cold molecular beams, as is commonly done in direct laser desorption [28]. Such experiments are underway in our laboratory and such a cold beam of intact large molecules would enable novel experiments, from controlling large molecules with external fields [29, 30] to direct diffractive imaging of single molecules in the gas-phase [18, 19].

Acknowledgments

This work has been supported by the European Research Council under the European Union’s Seventh Framework Programme (FP7/2007-2013) through the Consolidator Grant COMOTION (ERC-614507-Küpper), by the excellence cluster “The Hamburg Center for Ultrafast Imaging – Structure, Dynamics and Control of Matter at the Atomic Scale” of the Deutsche Forschungsgemeinschaft (CUI, DFG-EXC1074), and by the Helmholtz Gemeinschaft through the “Impuls- und Vernetzungsfond”. Z. H. gratefully acknowledges a scholarship of the Joachim-Herz-Stiftung and financial support from the PIER Helmholtz Graduate School.

References

- [1] B. Lindner, U. Seydel, Laser desorption mass spectrometry of nonvolatiles under shock wave conditions, *Anal. Chem.* 57 (1985) 895–899. doi:10.1021/ac00281a027. URL <http://pubs.acs.org/doi/abs/10.1021/ac00281a027>
- [2] C. R. Calvert, L. Belshaw, M. J. Duffy, O. Kelly, R. B. King, A. G. Smyth, T. J. Kelly, J. T. Costello, D. J. Timson, W. A. Bryan, T. Kierspel, P. Rice, I. C. E. Turcu, C. M. Cacho, E. Springate, I. D. Williams, J. B. Greenwood, LIAD-fs scheme for studies of ultrafast laser interactions with gas phase biomolecules, *Phys. Chem. Chem. Phys.* 14 (18) (2012) 6289–6297. doi:10.1039/c2cp23840c. URL <http://dx.doi.org/10.1039/c2cp23840c>
- [3] L. Belshaw, F. Calegari, M. J. Duffy, A. Trabattoni, L. Poletto, M. Nisoli, J. B. Greenwood, Observation of ultrafast charge migration in an amino acid, *J. Phys. Chem. Lett.* 3 (24) (2012) 3751–3754. doi:10.1021/jz3016028. URL <http://pubs.acs.org/doi/abs/10.1021/jz3016028>
- [4] F. Calegari, D. Ayuso, A. Trabattoni, L. Belshaw, S. De Camillis, S. Anumula, F. Frassetto, L. Poletto, A. Palacios, P. Decleva, J. B. Greenwood, F. Martín, M. Nisoli, Ultrafast electron dynamics in phenylalanine initiated by attosecond pulses, *Science* 346 (6207) (2014) 336–339. doi:10.1126/science.1254061. URL <http://science.sciencemag.org/content/346/6207/336.full>

- [5] Z. Huang, T. Ossenbrüggen, I. Rubinsky, M. Schust, D. A. Horke, J. Küpper, Development and characterization of a laser-induced acoustic desorption source, *Anal. Chem.* 90 (6) (2018) 3920–3927. arXiv:1710.06684, doi:10.1021/acs.analchem.7b04797.
URL <http://pubs.acs.org/doi/10.1021/acs.analchem.7b04797>
- [6] R. C. Shea, S. C. Habicht, W. E. Vaughn, H. I. Kenttämäa, Design and characterization of a high-power laser-induced acoustic desorption probe coupled with a fourier transform ion cyclotron resonance mass spectrometer, *Anal. Chem.* 79 (7) (2007) 2688–2694. doi:10.1021/ac061597p.
URL <http://pubs.acs.org/doi/abs/10.1021/ac061597p>
- [7] R. C. Shea, C. J. Petzold, J. L. Campbell, S. Li, D. J. Aaserud, H. I. Kenttämäa, Characterization of laser-induced acoustic desorption coupled with a fourier transform ion cyclotron resonance mass spectrometer, *Anal. Chem.* 78 (17) (2006) 6133–6139. doi:10.1021/ac0602827.
URL <http://pubs.acs.org/doi/abs/10.1021/ac0602827>
- [8] S. C. Habicht, L. M. Amundson, P. Duan, N. R. Vinuesa, H. I. Kenttämäa, Laser-induced acoustic desorption coupled with a linear quadrupole ion trap mass spectrometer, *Anal. Chem.* 82 (2) (2010) 608–614. doi:10.1021/ac901943k.
URL <http://pubs.acs.org/doi/abs/10.1021/ac901943k>
- [9] W.-P. Peng, Y.-C. Yang, M.-W. Kang, Y.-K. Tzeng, Z. Nie, H.-C. Chang, W. Chang, C.-H. Chen, Laser-induced acoustic desorption mass spectrometry of single bioparticles, *Angew. Chem. Int. Ed.* 45 (2006) 1423–1426. doi:10.1002/anie.200503271.
URL <http://onlinelibrary.wiley.com/doi/10.1002/anie.200503271/abstract>
- [10] N. Zhang, K. Zhu, C. Xiong, Y. Jiang, H.-C. Chang, Z. Nie, Mass measurement of single intact nanoparticles in a cylindrical ion trap, *Anal. Chem.* 88 (11) (2016) 5958–5962. doi:10.1021/acs.analchem.6b00918.
URL <http://pubs.acs.org/doi/abs/10.1021/acs.analchem.6b00918>
- [11] V. V. Golovlev, S. L. Allman, W. R. Garrett, N. I. Taranenko, C. H. Chen, Laser-induced acoustic desorption, *Int. J. Mass Spectrom. Ion Processes* 169–170 (1997) 69–78. doi:10.1016/S0168-1176(97)00209-7.
URL <http://linkinghub.elsevier.com/retrieve/pii/S0168117697002097>
- [12] A. Dow, A. Wittrig, H. Kenttämäa, Laser-induced acoustic desorption (liad) mass spectrometry, *Eur. J. Mass Spectrom.* 18 (2) (2012) 77–92. doi:10.1255/ejms.1162.
URL http://www.impublications.com/content/abstract?code=E18_0077
- [13] L. Nyadong, J. P. Quinn, C. S. Hsu, C. L. Hendrickson, R. P. Rodgers, A. G. Marshall, Atmospheric pressure laser-induced acoustic desorption chemical ionization mass spectrometry for analysis of saturated hydrocarbons, *Anal. Chem.* 84 (16) (2012) 7131–7137. doi:10.1021/ac301307p.
URL <http://pubs.acs.org/doi/abs/10.1021/ac301307p>
- [14] R. C. Shea, C. J. Petzold, J.-a. Liu, H. I. Kenttämäa, Experimental investigations of the internal energy of molecules evaporated via laser-induced acoustic desorption into a fourier transform ion cyclotron resonance mass spectrometer, *Anal. Chem.* 79 (5) (2007) 1825–1832. doi:10.1021/ac061596x.
URL <http://pubs.acs.org/doi/abs/10.1021/ac061596x>
- [15] N. J. Demarais, Z. Yang, T. P. Snow, V. M. Bierbaum, Gas-phase reactions of polycyclic aromatic hydrocarbon cations and their nitrogen-containing analogs with h atoms, *Astrophys. J.* 784 (1) (2014) 25–7. doi:10.1088/0004-637X/784/1/25.
URL <http://stacks.iop.org/0004-637X/784/i=1/a=25?key=crossref.35f76738aeb2c9005ab459833a5c32ae>
- [16] U. Sezer, L. Wörner, J. Horak, L. Felix, J. Tüxen, C. Götz, A. Vaziri, M. Mayor, M. Arndt, Laser-induced acoustic desorption of natural and functionalized biochromophores, *Anal. Chem.* 87 (11) (2015) 5614–5619. doi:10.1021/acs.analchem.5b00601.
URL <http://pubs.acs.org/doi/abs/10.1021/acs.analchem.5b00601>
- [17] U. Sezer, P. Schmid, L. Felix, M. Mayor, M. Arndt, Stability of high-mass molecular libraries: the role of the oligoporphyrin core, *J. Mass. Spectrom.* 50 (2015) 235–239. doi:10.1002/jms.3526.
URL <http://doi.wiley.com/10.1002/jms.3526>
- [18] A. Barty, J. Küpper, H. N. Chapman, Molecular imaging using x-ray free-electron lasers, *Annu. Rev. Phys. Chem.* 64 (1) (2013) 415–435. doi:10.1146/annurev-physchem-032511-143708.
URL <http://dx.doi.org/10.1146/annurev-physchem-032511-143708>
- [19] J. Küpper, S. Stern, L. Holmegaard, F. Filsinger, A. Rouzée, A. Rudenko, P. Johnsson, A. V. Martin, M. Adolph, A. Aquila, S. Bajt, A. Barty, C. Bostedt, J. Bozek, C. Caleman, R. Coffee, N. Coppola, T. Delmas, S. Epp, B. Erk, L. Foucar, T. Gorkhover, L. Gumprecht, A. Hartmann, R. Hartmann, G. Hauser, P. Holl, A. Hömke, N. Kimmel, F. Krasniqi, K.-U. Kühnel, J. Maurer, M. Messerschmidt, R. Moshhammer, C. Reich, B. Rudek, R. Santra, I. Schlichting, C. Schmidt, S. Schorb, J. Schulz, H. Soltau, J. C. H. Spence, D. Starodub, L. Strüder, J. Thøgersen, M. J. J. Vrakking, G. Weidenspointner, T. A. White, C. Wunderer, G. Meijer, J. Ullrich, H. Stapelfeldt, D. Rolles, H. N. Chapman, X-ray diffraction from isolated and strongly aligned gas-phase molecules with a free-electron laser, *Phys. Rev. Lett.* 112 (2014) 083002. arXiv:1307.4577, doi:10.1103/PhysRevLett.112.083002.
URL <https://dx.doi.org/10.1103/PhysRevLett.112.083002>
- [20] X.-J. Wang, J.-Z. You, Study on the molecular structure and thermal stability of purine nucleoside analogs, *J. Anal. Appl. Pyrolysis* 111 (2015) 1–14. doi:10.1016/j.jaap.2014.12.024.
URL <http://linkinghub.elsevier.com/retrieve/pii/S016523701400374X>
- [21] V. Y. Yablokov, I. L. Smel'tsova, I. A. Zelyaev, S. V. Mitrofanova, Studies of the rates of thermal decomposition of glycine, alanine, and serine, *Russ. J. Gen. Chem.* 79 (8) (2009) 1704–1706. doi:10.1134/S1070363209080209.
URL <http://link.springer.com/10.1134/S1070363209080209>
- [22] A. V. Zinovev, I. V. Veryovkin, J. F. Moore, M. J. Pellin, Laser-driven acoustic desorption of organic

- molecules from back-irradiated solid foils, *Anal. Chem.* 79 (21) (2007) 8232–8241. doi:10.1021/ac070584o.
 URL <http://pubs.acs.org/doi/abs/10.1021/ac070584o>
- [23] D. P. DePonte, U. Weierstall, K. Schmidt, J. Warner, D. Starodub, J. C. H. Spence, R. B. Doak, Gas dynamic virtual nozzle for generation of microscopic droplet streams, *J. Phys. D* 41 (19) (2008) 195505. doi:10.1088/0022-3727/41/19/195505.
 URL <http://iopscience.iop.org/0022-3727/41/19/195505>
- [24] K. R. Beyerlein, L. Adriano, M. Heymann, R. Kirian, J. Knoska, F. Wilde, H. N. Chapman, S. Bajt, Ceramic micro-injection molded nozzles for serial femtosecond crystallography sample delivery, *Rev. Sci. Instrum.* 86 (12) (2015) 125104–12. doi:10.1063/1.4936843.
 URL <http://dx.doi.org/10.1063/1.4936843>
- [25] P. J. Linstrom, W. G. Mallard (Eds.), NIST Chemistry WebBook, NIST Standard Reference Database Number 69, National Institute of Standards and Technology, Gaithersburg MD, 20899, 2017. doi:10.18434/T4D303.
 URL <http://webbook.nist.gov>
- [26] A. Bondi, Thermal properties of molecular crystals. I. Heat capacity and thermal expansion, *J. Appl. Phys.* 37 (13) (1966) 4643–4647. doi:10.1063/1.1708111.
 URL <http://aip.scitation.org/doi/10.1063/1.1708111>
- [27] N. R. Hutzler, H.-I. Lu, J. M. Doyle, The buffer gas beam: An intense, cold, and slow source for atoms and molecules, *Chem. Rev.* 112 (9) (2012) 4803–4827. doi:10.1021/cr200362u.
 URL <http://pubs.acs.org/doi/abs/10.1021/cr200362u>
- [28] N. Teschmit, K. Długołęcki, D. Gusa, I. Rubinsky, D. A. Horke, J. Küpper, Characterizing and optimizing a laser-desorption molecular beam source, *J. Chem. Phys.* 147 (2017) 144204. arXiv:1706.04083, doi:10.1063/1.4991639.
 URL <http://dx.doi.org/10.1063/1.4991639>
- [29] Y.-P. Chang, D. A. Horke, S. Trippel, J. Küpper, Spatially-controlled complex molecules and their applications, *Int. Rev. Phys. Chem.* 34 (2015) 557–590. arXiv:1505.05632, doi:10.1080/0144235X.2015.1077838.
 URL <http://dx.doi.org/10.1080/0144235X.2015.1077838>
- [30] N. Teschmit, D. A. Horke, J. Küpper, Spatially separating the conformers of the dipeptide Ac-Phe-Cys-NH₂, *Angew. Chem. Int. Ed.* 57 (42) (2018) 13775–13779. arXiv:1805.12396, doi:10.1002/anie.201807646.
 URL <https://onlinelibrary.wiley.com/doi/abs/10.1002/anie.201807646>